

A new study regarding the comparison of calculated and measured RSSI values under different experimental conditions

Abstract. This paper presents a new detailed study of comparison measured Received Signal Strength Indicator (RSSI) values, with the values being calculated by two electromagnetic (EM) wave propagation models, log-normal, and two ray ground-reflection models, respectively. Different experimental conditions were considered. We used different numbers of transmitting and receiving antennas, antennas geometrical placement and orientations-polarizations. This study was performed for long-range and short-range measurements inside and outside buildings.

Streszczenie. W artykule porównano metody pomiaru współczynnika RSSI (wskaźnik siły otrzymanego sygnału) dla dwóch modeli propagacji fali elektromagnetycznej. Stosowane różne warunki – różną liczbę anten, różne położenie anten i różne polaryzacje. (Studium porównawcze obliczania i pomiar współczynnika RSSI w różnych warunkach)

Keywords: EM propagation models. Received Signal Strength Indicator (RSSI). Wireless Sensor Network.

Słowa kluczowe: propagacja fali elektromagnetycznej, współczynnik RSSI, anteny, bezprzewodowa sieć czujników.

Introduction

Wireless sensor network (WSN) has become a very interesting research topic over the last few years. Recent advances in micro-electro-mechanical systems technology, wireless communications, and digital electronics have enabled the development of low-cost sensor nodes capable of communicating with each other over short distances [1]. These small nodes consist of only a few components: the radio part for spreading data, the sensor part for sensing environmental phenomena, the processing unit and the power supply. There are many active applications where WSN can be used: from military applications to healthcare and environmental monitoring. Usually data from a sensor field data are collected at a base station, but this data are meaningless without positional information. Because of this, the node location or positional estimation has become a very interesting research topic over the last few years [2-4]. Positional estimation facilitates applications such as inventory tracking, intruder detection, the tracking of firefighters or miners, home automation, and patient monitoring. These potential applications for wireless location estimation have also been recognized by IEEE, which has set-up a standardization group 802.15.4a for designing a new physical layer for low-data rate communications combined with positioning capabilities [5].

There are several techniques for determining the distances between nodes. Physically, the following can be measured: the time of the radio frequency (RF) signal arrival (TOA), the angle of signal arrival (AOA) or the received power of the signal, i.e. RSSI.

Most 802.11 and 802.15.4 radio modules support the measurement of RSSI. RSSI is measured for each received packet. The power or energy of a signal travelling between two nodes (transmitting and receiving) is a signal parameter which can be used for distance estimation, together with path-loss and shadowing model. Within a free-space environment, RSSI can be used for estimating the locations of other nodes placed on a circle with radius r . RSSI measurements are very unpredictable because there are many sources of uncertainty [6]. Within free space, the received power is reciprocal to the square of the distance between nodes i and j , respectively.

The measuring the time of arrival is costly. The TOA technique demands very accurate and expensive time synchronization between all nodes within the network. TDOA measures the time difference of arrival between a node and two anchors.

Also the AOA of the signal can be measured [7]. With this parameter we can obtain directions to neighbouring

sensors. Belonging hardware is more expensive than the hardware for RSSI estimation.

The important fact about WSNs is the price per sensor node because there are usually more than ten or up to a few thousand sensors. Only the anchor or reference nodes, therefore, are usually equipped with a GPS module to determine absolute position.

On chip RSSI-measurements offer cheap solutions for distance measurements between nodes in wireless sensor networks. The presented work covers the results of our new detailed study of comparison of calculated and measured RSSI values under different experimental conditions. The goal of our detailed study is further using obtained results for improving localization applications.

The rest of this paper is organized as follows. Section 2 describes the EM waves propagation law, and the models are described together with their applicability for WSNs localization. Section 3 presents the results of RSSI measurements under different experimental conditions and comments. The final discussion of results is provided in section 4.

EM propagation law and models

Knowledge about the propagation of electromagnetic waves is very important in wireless communications. In theory, the strength of a signal decays with every square of length, but only in a vacuum without an obstacle. In practice, things are more complicated. In real-world channels, multipath signals and shadowing are major sources of environmental dependence when measuring RSSI. Multiple signals with different amplitudes and phases arrive at the receiver, and these signals are added constructively or destructively as a function of the frequency. These shadowing effects are random.

There are many known radio propagation models for wireless communications that predict signal-strength loss with distance and path loss. We will review two models here, the log normal and the two rays or ground reflection models, respectively. Later we will study their matching with measurements and usefulness in practical applications.

An open field is one of the simplest and most commonly used environments to do RF range testing. The propagation of radio communication is generally described by the Friis equation [8-16]. This equation describes the dependency between distance, frequency (2.4 GHz), antennas gain, transmitted and received power:

$$(1) \quad P_r = P_t \frac{G_t G_r \lambda^2}{(4\pi)^2 d^n} ; \quad n = 2..4$$

where P_r is the power available from the receiving antenna, P_t is the power supplied to the transmitting antenna, G_R is gain in the receiving antenna, G_T is the gain of the transmitting antenna, λ is the wavelength of the RF signal, d is the distance and n is the path-loss exponent, typically between 2 and 4.

The log-normal propagation model is the modification of the Friis ideal equation, usually used in real-world:

$$(2) \quad \bar{P}_0(d) = P_0(d_0) - 10n \log\left(\frac{d}{d_0}\right)$$

where $\bar{P}(d)$ is the average received power in dB at distance d , P_0 is the received power in dB at a short reference distance d_0 , $d_0 < d$. The advantage of this model is, that some parameters of the transmitter and receiver (P_T , G_T , G_R , λ) are eliminated by normalization with reference values.

Another interesting and often used model is the so-called two ray or ground reflection model [8, 9]. Fig. 1 shows the idealized scenario with an infinite, perfectly flat ground plane and no other objects obstructing the signal. The total received power (energy) can be modelled as the vector sum of directly transmitted waves, and one ground-reflected wave. The radio signal is never 100% reflected from the ground. One portion of the energy is reflected and the other passes through the junction. The portion of the reflected signal depends on the wave polarization (vertical or horizontal), incident angle Θ_i and the different electrical constants of the surface (ϵ_r - dielectric constant, μ_r - magnetic permeability, δ - conductivity). The Fresnel reflection coefficients for the vertical (Γ_v) and horizontal (Γ_h) polarized signals are calculated by equations (3) and (4), respectively, which assume that both substances (air and soil) have equal permeability $\mu \approx 1$:

$$(3) \quad \Gamma_v = \frac{(\epsilon_r - j60\sigma\lambda) \sin \Theta_i - \sqrt{\epsilon_r - j60\sigma\lambda - \cos^2(\Theta_i)}}{(\epsilon_r - j60\sigma\lambda) \sin \Theta_i + \sqrt{\epsilon_r - j60\sigma\lambda - \cos^2(\Theta_i)}}$$

$$(4) \quad \Gamma_h = \frac{\sin \Theta_i - \sqrt{\epsilon_r - j60\sigma\lambda - \cos^2(\Theta_i)}}{\sin \Theta_i + \sqrt{\epsilon_r - j60\sigma\lambda - \cos^2(\Theta_i)}}$$

We used typical electrical data [8] for the soil: $\delta=0,005$ m Ω /m and $\epsilon_r=15$ for average soil.

Equations (5) to (17) derive at a 2-ray reflection model for geometry, as given in Fig. 1:

$$(5) \quad D = \sqrt{(H_2 - H_1)^2 + d^2}$$

$$(6) \quad R = \sqrt{(H_1 + H_2)^2 + d^2}$$

$$(7) \quad \Theta_i = \arctan\left(\frac{H_1 + H_2}{d}\right)$$

The phase difference Δ between the direct and ground-reflected waves is:

$$(8) \quad \Delta = \frac{2\pi}{\lambda}(R - D)$$

The equation of received power P_R at the receiver must be derived from electric field [15]:

$$(9) \quad \vec{E}_R = \vec{E}_{direct} + \vec{E}_{reflect}$$

Where received electric field at the receiver \vec{E}_R is vector sum of direct and reflected electric field at the receiver, \vec{E}_{direct} and $\vec{E}_{reflect}$, respectively.

$$(10) \quad E_{reflect} = E_{direct} \cdot \Gamma e^{-j\Delta}$$

$$(11) \quad E_R = E_{direct} (1 + \Gamma e^{-j\Delta})$$

$$(12) \quad \Gamma = |\Gamma| e^{-j\psi}$$

$$(13) \quad E_R = E_{direct} (1 + |\Gamma| e^{-j(\Delta - \psi)})$$

In our case, where $\Gamma \approx 1$, we can write:

$$(14) \quad E_R = E_{direct} (1 - e^{-j\Delta}) = E_{direct} (1 - \cos \Delta + j \sin \Delta)$$

$$(15) \quad |E_R| = 2 \left| E_{direct} \sin \frac{\Delta}{2} \right|$$

Received power P_R is proportional E_R^2 :

$$(16) \quad P_R \propto 4 |E_{direct}|^2 \sin^2 \left(\frac{2\pi H_1 H_2}{\lambda d} \right)$$

$$(17) \quad P_R \propto 4 P_T \left(\frac{\lambda}{4\pi d} \right)^2 G_T G_R \sin^2 \left(\frac{2\pi H_1 H_2}{\lambda d} \right)$$

Where Γ is the Fresnel coefficient from (3) or (4), D is the path-length of the direct transmission, R is the length of the reflected transmission, Δ is the phase difference and d is distance between transceivers.

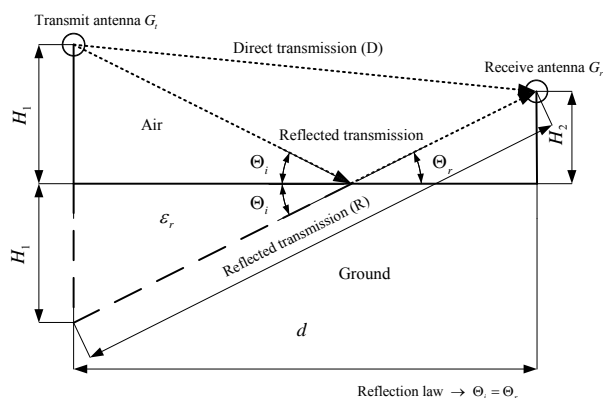


Fig. 1. Ground reflection model

During typical radio transmission, the waves are reflected and obstructed by all objects illuminated by the transmitting antenna.

Measuring of parameter RSSI with comments

RSSI is the measured power of the received radio signal and its measurement is implemented and widely used in 802.11 standards. Measurements of RSSI were performed on radio module CC2500 [11, 16 and 17] attached onto the SPaRCMosquito platform developed in our laboratory [18]. Microstrip dipole antenna is directly connected to module CC2500 with no need of impedance matching. This is one of major advantages of microstrip antennas, beside easy implementation. More details about used microstrip antenna can be found in [19]. The output power of a radio module is about 1 mW (0 dBm). We assumed the gain of antennas is approximately 1. When a received signal is demodulated and decoded, the radio module mechanism attaches the measured power of input signal, known as RSSI, to every received packet. RSSI is an 8-bit hexadecimal number and must be converted to dBm. Conversion, depending on the manufacturer of the radio module, is usually linear.

Measurement at long distances

We took two major sets of measurements: i) inside a building and ii) outside in an open field.

We setup different types of digital modulations and bit-rates on radio chips CC2500 and RSSI were measured at different predefined distances (1, 2, ..., 40 m in an underground garage and 1, 2, ..., 80 m in an open field). The captured data were processed using software Matlab® [20]. At each distance we took 20 RSSI-measurements and

averaged them in the Matlab program in order to decrease random fluctuations.

Measurements (1) were done inside a large underground garage with walls of reinforced concrete (Fig. 2).



Fig. 2. Inside testing area

The relationship between the obtained RSSI and the distance between the receiver and transmitter was measured at different scenarios: different altitudes from the ground, orientations-polarization, geometrical displacement, and number of transmitting and receiving nodes. We also measured at different modulation types (MSK, 2-FSK, GFSK, and OQPSK) and different bit rates (38 kb/s, 250 kb/s and 500 kb/s). As expected due to the fact that the largest EM effects were the reflections and diffractions, and the type of digital modulation and bit rate had little effect on the RSSI measurements (Fig. 3 and Fig. 4). At the highest bit-rate 500 kb/s, the communication was quickly interrupted at a relatively small distance of 20 m because of the achieved channel capacity limit.

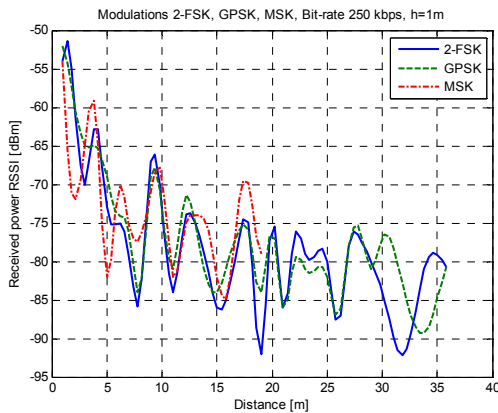


Fig. 3. Comparison of different modulations

A comparison between measured RSSI-values and simulated, is presented in Fig. 5. The accuracy of two-ray model is better for distances from approximately 3 m to 20 m. RSSI was dependent on the altitudes of the receiver and transmitter. The closer to the floor the nodes were, the lower were the deviations of the measurements from the theoretical values calculated by the log-normal propagation model (2). Namely, the time difference between the floor reflected signal and the direct signal was smaller in this case (Fig. 6). At higher altitudes the two-ray model was more accurate for distances of approximately 5 to 20 m.

Another set of measurements (2) were taken outside in a meadow (Fig. 7), where the nodes were placed 1 m from the ground. We took measurements of the received power up to a distance of 90 m (CC2500 max range is about 100 m).

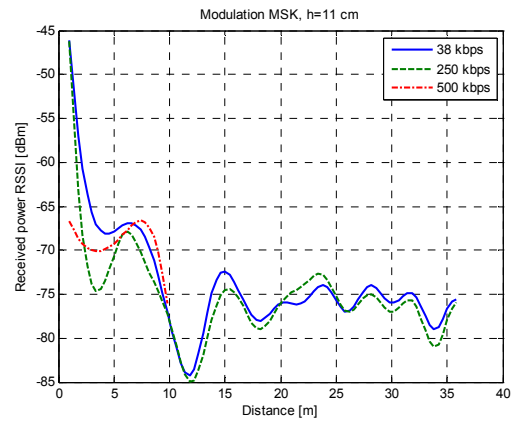


Fig. 4. RSSI at different bit-rates (38 kb/s, 250 kb/s, and 500 kb/s)

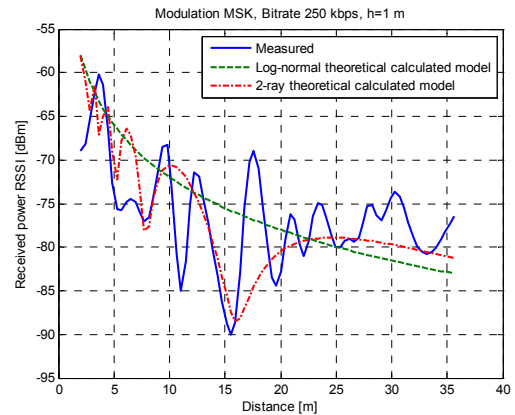


Fig. 5. Calculated propagation models (log-normal and 2-ray ground reflected) vs. Measured

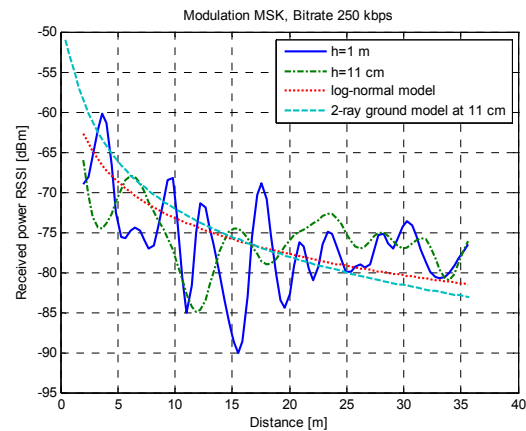


Fig. 6 Received power at two different altitudes from ground

Fig. 8 and Fig. 9 show the curves RSSI vs. distance for the two ray ground model (17), log-normal model (2), and the measured values. MSK modulation was used in Fig. 8 and 2-FSK in Fig. 9. The bit-rate was 250 kbps in both cases. Reasonably good matching could be seen between the theoretical and measured values for both models. As expected the type of modulation and the bit rate did not significantly influence on matching the measurement with models. It could be observed that the 2-ray, i.e. ground reflection model better matched with the measurements than the log-normal model with $n=2$. The value n was obtained experimentally to best match the measurements using the Least Mean Square method (LMS).

The presence of a human body within the measurement field had a significant influence on the measurement results. The measurements at each distance point were, in our case, done without a human's body present. In a rural

environment there was significantly smaller probability of interference from other 2.4 GHz signals.



Fig. 7. Outside testing area

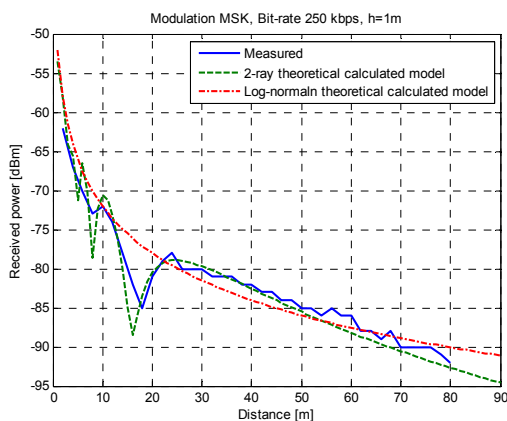


Fig. 8. Two-ray ground reflection and log-normal model and measurements, MSK-modulation

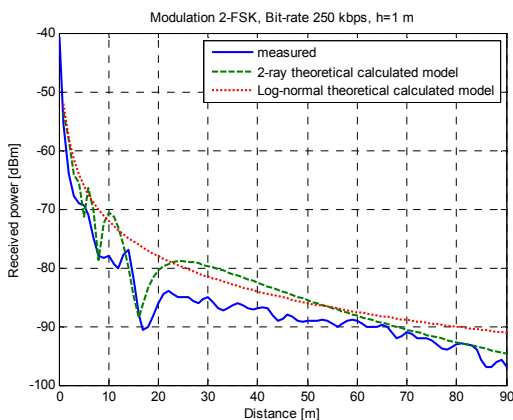


Fig. 9. Same as in Fig. 8 and 2-FSK modulation

Measurements at short distances within a small room

The next set of measurements was carried-out in the laboratory with dimensions 10 m x 5 m x 3 m. Measurements of RSSI at small distances in small rooms are also important due to many possible applications as for example navigation of very small vehicles, mobile robots or localization applications for monitoring old people or children.

Sending and receiving nodes were placed at small altitudes, approximately 3 cm from the floor. The receiving node was moved along over predefined distances. About 20 measurements were carried out at each position and averaged using Matlab program in order to reduce random fluctuations. Averaging of measured RSSI-curves for the

two receiving antennas was also performed in the Matlab program. The distances were chosen between zero and 3 metres. It should be noted that, for lower transmitter altitudes the ground model (2-ray) provided practically the same results as the log-normal, because of the small impact of a ground-reflected signal. We performed different RSSI measurement cases.

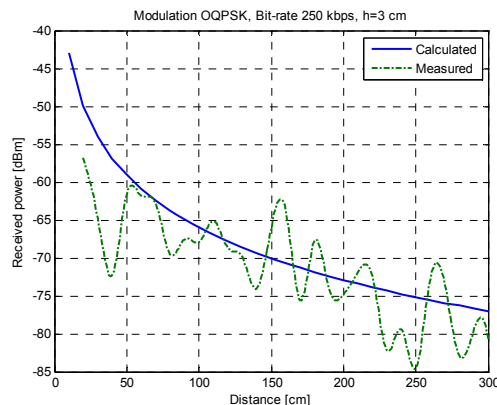


Fig. 10. Calculated log-normal propagation model measured

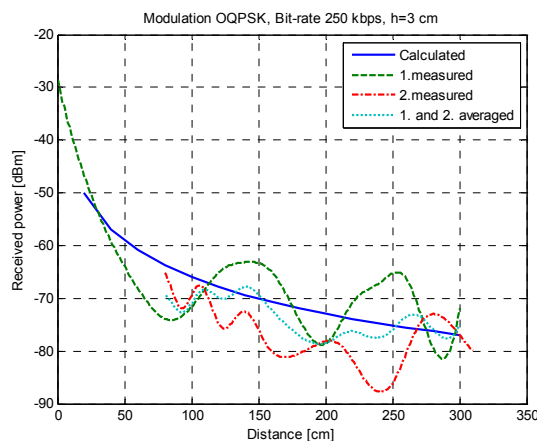


Fig. 11. Measurements from three nodes placed on right-angle triangle

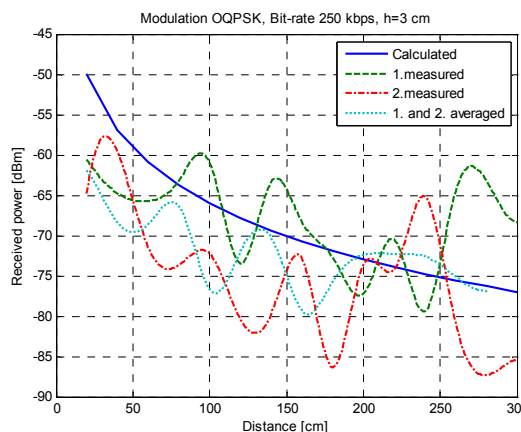


Fig. 12. Three nodes placed on isosceles triangle

Two nodes were used in the first case, one static transmitting node and one mobile receiving node. Fig. 10 shows the measured values versus the theoretical values calculated with a log-normal model ($n=2.3$) using equation (2). The value n was obtained experimentally to best match the measurements using LMS. The measurement curve is quite accurate with ripples of approximately 10 dB.

We used three nodes in the second case. Two were static

transmission nodes, and one a mobile receiving node placed in the direction of the second cachet of a right-angled triangle. The distance between static nodes was known (40 cm). By averaging the two measured curves, a smoother power curve was again obtained (Fig. 11).

The next experiment was performed again with two static nodes and one mobile node, but placed on the line in the direction of an isosceles triangle (Fig. 12). The measurement curves again followed the log-normal model but the ripple was little stronger with peak amplitudes of about 10 to 15 dB. The differences in the case of Fig. 11 can be explained by the different geometrical placements of the transmitters and the receiver. The ripple was also reduced by averaging the obtained curves.

Next two received nodes were used, placed close to each other, exactly one on top of the another (Fig. 13).

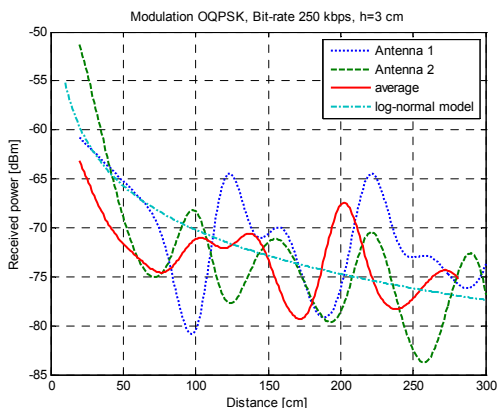


Fig. 13. Received power at two receiving antennas placed one on top of the another

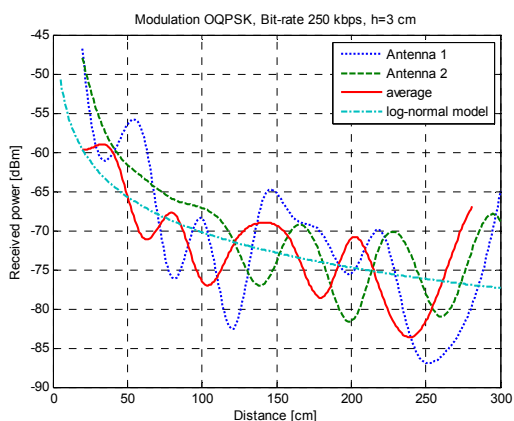


Fig. 14. Vertical and horizontal polarizations of the receiving antennas

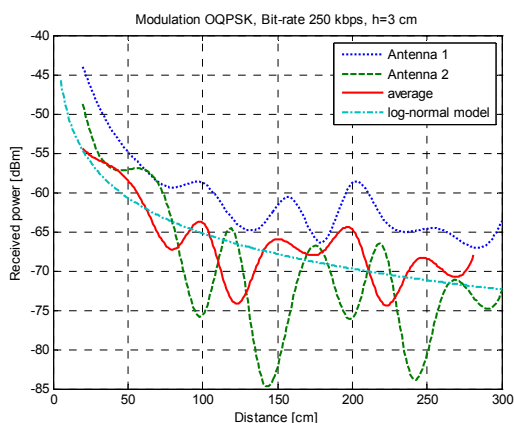


Fig. 15. Vertical polarized transmitter antenna

Fig. 14 shows the case where the upper antenna (node) from the previous case was rotated by 90° in a vertical direction (i.e one polarized in the horizontal and the other in the vertical direction). In Fig. 15 the transmitting antenna was polarized vertically and the receiving antennas were placed as in Fig. 14. The results of the measurements for the last three cases were similar as for the previous short distance measurements. The average of the two receiving antennas measurements were again computed using the Matlab program and the ripple was again reduced.

Relative deviation of propagation models from the measurements

The relative deviation of the measured data from the simulated EM wave propagation models (2) and (17) were evaluated, as presented in Fig. 16 to Fig. 18. The relative deviation of the estimated model was calculated using the equation:

$$(18) \text{ Relative deviation (\%)} = \left| \frac{P_{R \text{ modeled}} - P_{R \text{ measured}}}{P_{R \text{ measured}}} \right| \cdot 100\%$$

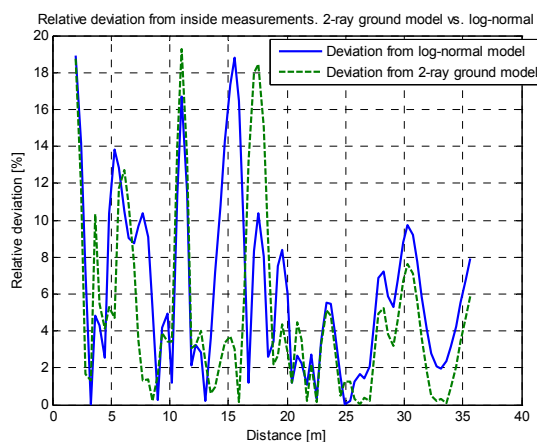


Fig. 16. Relative deviations for the measurements in Fig. 3

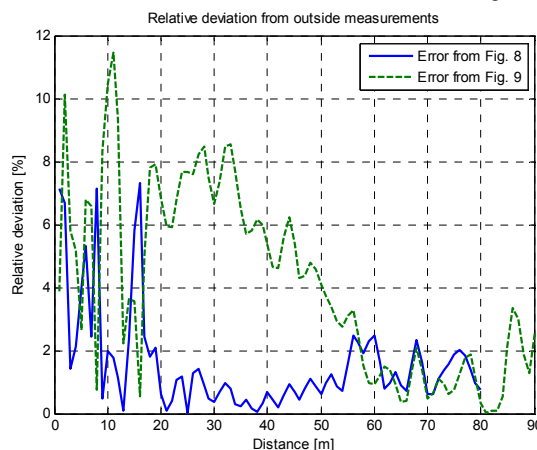


Fig. 17. Relative deviations for the measurements in Fig. 8 and Fig. 9

In the case of measurements carried out in the open field, we obtained smaller deviations (Fig. 17) in comparison with the inside measurements (Fig. 16). The relative deviations were, on average, approximately 11 % and 20 %, respectively. The greater measurement errors inside the building were explained as the reflections from the walls and various obstacles. The relative errors in both cases were calculated from the 2-ray reflection model (17).

The measured results at very short distances in small rooms gave us relative deviations from the log-normal model of up to 30 % (Fig. 18 and Fig. 19).

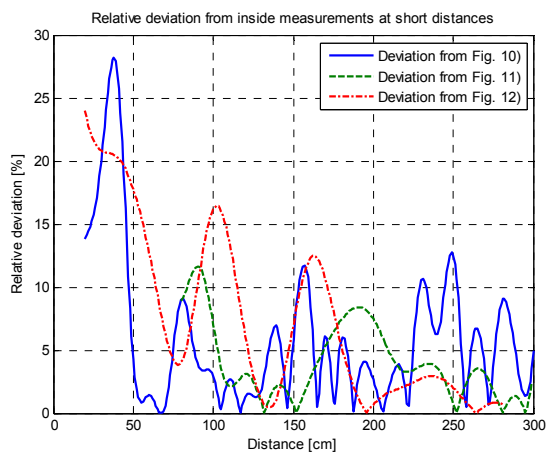


Fig. 18. Relative deviations from the measurements in Fig. 10, Fig. 11, and Fig. 12

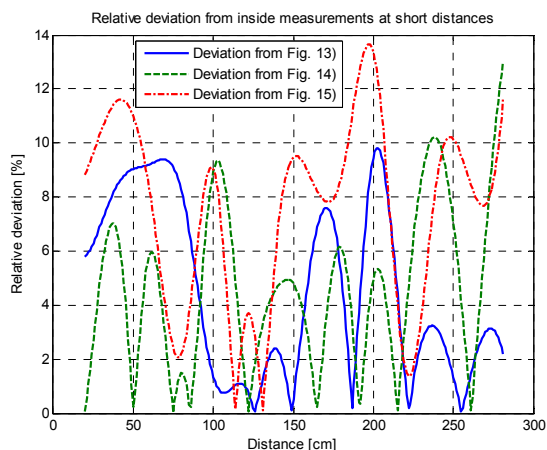


Fig. 19. Relative deviation from the measurements in Fig. 13, Fig. 14, and Fig. 15

Conclusion

RSSI deviation was, on average, about 15 % for inside measurements over short distances up to 400 cm using the log-normal model (Fig. 19).

For long-range outside measurements, the matching of RSSI with distance measurements was quite good, the deviations were about 5%, for those distances greater than 20 m for both models, the two-ray ground reflection model as well as the log-normal model. However, the two-ray model better matched regarding measurements, because it considered the ground reflected waves.

Additionally, we evaluated the influences of some other impact factors on the RSSI-measurement regarding the number of antennas, their orientation-polarization, and their (i.e. nodes) geometrical placements. We confirmed the expectations that the chosen digital modulation techniques and bit rates would not practically impact on the measured RSSI values. The sending and receiving antenna orientation and EM polarization significantly influenced the measured RSSI. The number of sending and receiving nodes and their positions was also important. By averaging the corresponding measured RSSI curves the ripples could be reduced and, as well as the deviations from log-normal model for the experimental conditions presented in this paper.

REFERENCES

- [1] Akyildiz, I. F., Su, W., Sankarasubramaniam, Y., Cayirci, E. (2002). Wireless sensor networks: a survey. *Computer Networks*, 38, 393-422.
- [2] Patwari, N., Hero, A.O., Perkins, M., Correal, N. S., O'Dea, R.J. (2003). Relative Location Estimation in Wireless Sensor Networks. *IEEE Transactions on Signal Processing*, 51(8).
- [3] Brida P., Machaj J., Gaborik F., Majer N., Performance analysis of positioning in wireless sensor networks, *Przegląd Elektrotechniczny*, 87 (2011), nr 5
- [4] Yubo Deng Y., Yang Y., Xiong2 Y., Li L, A displacement estimated localization algorithm in the opportunistic communication based wireless sensor network, *Przegląd Elektrotechniczny*, 89 (2013), nr 1b
- [5] Gezici, S. (2007). A Survey on Wireless Position Estimation. *Wireless Personal Communications*, 44(3), 262-282.
- [6] Benkic, K., Malajner, M., Planinsic, P., Cucej, Z. (2008). Using RSSI value for distance estimation in wireless sensor networks based on ZigBee. Proceedings of 15th International Conference on Systems, Signals and Image Processing, 303-306.
- [7] Patwari, N., et al. (2005). Locating the nodes: cooperative localization in wireless sensor networks. *Signal Processing Magazine*, 22(4), 54-69.
- [8] Barton, D. K. (1998). *Radar Technology Encyclopedia* (p. 394). Boston/London: Artech House. Inc.
- [9] Kvaksrud, T. (2008). Range Measurements in an Open Field Environment. <http://www.ti.com/lit/an/swra169a/swra169a.pdf>
- [10] Guolin Sun, Jie Chen, Wei Guo, and Liu K.J.R., "Signal processing techniques in network-aided positioning: a survey of state-of-the-art positioning designs," *Signal Processing Magazine*, vol. 22, no. 4, pp. 12-33, 2005.
- [11] Benkic, K., Malajner, M., Planinsic, P., Cucej, Z. (2009). The accuracy of propagation models for distance measurement between WSN nodes. Proceedings of 16th International Conference on System, Signals & Image Processing, 3.
- [12] Li, L. (2006). RSS-Based Location Estimation with Unknown Pathloss Model. *IEEE Transactions on Wireless Communications*, 5(12), 3626-3633.
- [13] Li, L. (2007). Collaborative Localization With Received-Signal Strength in Wireless Sensor Networks. *IEEE Transactions on Vehicular Technology* 56(6), 3807-3817.
- [14] Stoyanova, T., Kerasiotis, F., Prayati, A., Papadopoulos, G. (2009). Evaluation of impact factors on RSS accuracy for localization and tracking applications in sensor networks. *Telecommunication Systems*, 42, 235-248.
- [15] J. D. Parson. (2000). *The Mobile Radio Propagation Channel*. John Wiley & Sons.
- [16] Texas Instruments (2009). Low Power RF ICs - 2.4GHz - CC2500 - TI.com. <http://focus.ti.com/docs/prod/folders/print/cc2500.html>
- [17] Benkic, K., Malajner, M., Cucej, Z. (2007). Implementacija sprejemno/oddajnega modula CC2500 za uporabo v brezžičnih senzorskih omrežjih. Zbornik šestnajste mednarodne Elektrotehniške in računalniške konference ERK 2007, A, 140-143. Malajner, M., Bekic, K., Cucej, Z. (2008). Online programmable wireless sensor node for testing purpose. 50th International Symposium ELMAR, 2, 531-534.
- [18] Audun Andersen, Folded Dipole Antenna for CC25xx. Chipcon product of Texas Instruments. SWRA118, Design Note DN 004, Texas Instruments.
- [19] MathWorks - MATLAB and Simulink for Technical Computing. <http://www.mathworks.com/>

Authors: Marko Malajner, Faculty of electrical engineering and computer science, University of Maribor, Smetanova ulica 17, 2000 Maribor, E-mail: marko.malajner@uni-mb.si